

# Simplified Gentlest Ascent Dynamics for Saddle Points in Non-gradient Systems

Shuting Gu<sup>1, a)</sup> and Xiang Zhou<sup>2, b)</sup>

<sup>1)</sup>Department of Mathematics, City University of Hong Kong, Tat Chee Ave, Kowloon, Hong Kong SAR

<sup>2)</sup>Department of Mathematics, City University of Hong Kong, Tat Chee Ave, Kowloon, Hong Kong SAR

(Dated: July 3, 2018)

The gentlest ascent dynamics (GAD) (*Nonlinearity*, vol. 24, no. 6, p1831, 2011) is a continuous time dynamics coupling both the position and the direction variables to efficiently locate the saddle point with a given index. These saddle points play important roles in the activated process of the randomly perturbed dynamical systems. For index-1 saddle points in non-gradient systems, the GAD requires two direction variables to approximate the eigenvectors of the Jacobian matrix and its transpose, respectively, while in the gradient systems, these two directions collapse to be the single min mode of the Hessian matrix. In this note, we present a simplified GAD which only needs one direction variable even for non-gradient systems. This new method not only reduces computational cost for directions by half, but also can avoid inconvenient operations on the transpose of Jacobian matrix. We prove the same convergence property for the simplified GAD as for the original GAD. The motivation of our simplified GAD is its formal analogy to the Hamiltonian dynamics governing the exit dynamics when the system is perturbed by small noise. Several non-gradient examples are presented to demonstrate our method, including the two dimensional models and the Allen-Cahn equation in the presence of shear flow.

PACS numbers: 05.40, 05.70.Ln, 82.40.Bj

Keywords: saddle point, rare event, non-gradient system

## I. INTRODUCTION

Locating the saddle points has been of broad interest in many areas of scientific applications, especially for the understanding the exit process leaving from linearly stable states when a dynamical system is randomly perturbed. In computational chemistry<sup>18</sup>, one of the most important objects on the potential energy surface is the transition state which is the saddle point with index 1, *i.e.*, the unstable manifold is exactly one dimensional. Such transition states are the bottlenecks on the most probable transition paths between different local wells that describe the random hoppings on the potential surface. The steepest descent flow that minimizes the potential energy gives arise to gradient dynamical systems. For such gradient systems, a large amount of numerical methods have been developed to locate their saddle points, such as the eigenvector following method<sup>1</sup>, the dimer method<sup>10</sup> and the gentlest ascent dynamics(GAD)<sup>5,17</sup>, the iterative minimization algorithm<sup>7,8</sup> and others<sup>13,21</sup>.

While most of these methods were designed for the gradient systems, there are few of them applicable to the non-gradient systems, which arise from many models in biology and fluid dynamics<sup>19,20</sup>. One prominent

example<sup>11,14</sup> is the phase field model such as the Allen-Cahn equation associated with a double-well potential, but subject to the influence of shear flow. The extra forcing from the fluid certainly makes the gradient system become a non-gradient model. The saddle points in such non-gradient systems are still of great importance since they may be also relevant to the non-equilibrium process in the randomly perturbed dynamical systems<sup>6</sup>.

Among many saddle search methods mentioned previously, only the GAD<sup>5</sup> proposed by one of the authors in this note is capable to address the saddle point in general dynamical systems, by using two eigenvectors and oblique projection. This result extends the saddle point search method to the non-gradient systems. In this note, we present a new form of the gentlest ascent dynamics associated with the following non-gradient system

$$\dot{x} = b(x), \quad (1)$$

where  $b$  is a smooth vector field in  $\mathbb{R}^d$ . We are interested in the index-1 saddle point of the vector field  $b$ . To locate the index-1 saddle point in equation (1), the original GAD<sup>5</sup> evolves a position variable  $x$  and two direction variables  $v$  and  $w$  so that the linearly stable state states of this new dynamics are index-1 saddle point of  $b$ . The dynamics of  $v$  and  $w$  in the GAD needs the product of the Jacobian matrix  $Db(x)$  and its transpose  $Db(x)^\top$  with  $v$  and  $w$ , respectively. The matrix-vector multiplication  $Db(x)v = \lim_{h \rightarrow 0}(b(x + hv) - b(x))/h$  can be easily approximated by the finite difference method. But the difficult comes from the calculation of the transposed term  $Db(x)^\top w$ , which lacks the interpretation of the di-

<sup>a)</sup>Electronic mail: shutinggu2-c@my.cityu.edu.hk

<sup>b)</sup>Electronic mail: xiang.zhou@city.edu.hk; Corresponding author.  
The research of XZ was supported by the grants from the Research Grants Council of the Hong Kong Special Administrative Region, China (Project No. CityU 11304715 and 11337216).

rectional derivative of  $b(x)$ . In our simplified GAD below, we shall show that it suffices to use the dynamics of *one* directional variable (either  $v$  or  $w$ ), without affecting the convergence property of the original GAD.

Despite the simple form of our result, we find an interesting connection between the simplified GAD and the underlying Hamilton's equation describing the optimal transition path in the randomly perturbed equation:

$$dX = b(X)dt + \sqrt{\varepsilon}dW, \quad (2)$$

where  $W$  is the standard Brownian motion and  $\varepsilon$  is a small constant. Indeed, the study of rare events in the system (2) is the most important motivation to study the saddle points of the vector field  $b$ . By the Freidlin-Wentzell large deviation theory<sup>6</sup>, the most probable transition path is a minimizer of the Freidlin-Wentzell action functional and this path, as a function of time, satisfies the Hamilton's equation with the zero Hamiltonian. The position and momentum in the Hamilton's equation might be thought as the counterpart of the position and direction in the GAD. This formal analogy is indeed our original inspiration to derive our simplified GAD.

The rest of the paper is organized as follows. In Section II, we propose the simplified GAD for non-gradient systems after a short review of the GAD. Then we explore the relation between the simplified GAD and the Hamilton's dynamics. In addition, we apply the simplified GAD to the multiscale model of non-gradient slow-fast systems. Section III is our numerical examples. In particular, we study the Allen-Cahn equation in the presence of shear flow and investigate how the shear rate affects the transitions states in this system. The conclusions and discussions are given in Section IV.

## II. METHOD

### A. Review of Gentlest Ascent Dynamics (GAD)

The GAD in<sup>5</sup> for the flow  $\dot{x}(t) = b(x)$  involves a position variable  $x$  and two direction variables  $v$  and  $w$  as follows:

$$\begin{cases} \dot{x}(t) = b(x) - 2 \frac{\langle b(x), w \rangle}{\langle w, v \rangle} v, \\ \gamma \dot{v}(t) = J(x)v - \alpha v, \end{cases} \quad (3a)$$

$$\gamma \dot{w}(t) = J(x)^T w - \beta w, \quad (3b)$$

$$(3c)$$

where  $J(x) = Db(x)$  is the Jacobian matrix  $(Db)_{ij} \doteq \frac{\partial b_i}{\partial x_j}$ , which is generally asymmetric.  $\alpha$  and  $\beta$  are the Lagrangian multipliers to impose certain normalization conditions for  $v$  and  $w$ . For instance, if the normalization condition is  $\langle v, v \rangle \equiv \langle w, w \rangle \equiv 1$ , then  $\alpha = \langle v, J(x)v \rangle$  and  $\beta = 2 \langle w, J(x)v \rangle - \alpha$ . Equation (3) is a flow in  $\mathbb{R}^{3d}$ .

As a special case, the GAD for a gradient system  $\dot{x}(t) = -\nabla V(x)$  only involves  $v$ :

$$\begin{cases} \dot{x}(t) = -\nabla V(x) + 2 \frac{\langle \nabla V(x), v \rangle}{\langle v, v \rangle} v, \end{cases} \quad (4a)$$

$$\gamma \dot{v}(t) = -\nabla^2 V(x)v + \langle v, \nabla^2 V(x)v \rangle v. \quad (4b)$$

$\gamma > 0$  is the relaxation parameter. A large  $\gamma$  means a fast relaxation for the direction variable  $v(t)$  toward to the steady state. For a frozen  $x$ , this steady state is the min mode of the Hessian  $\nabla^2 V(x)$ : the eigenvector corresponding to the smallest eigenvalue of  $\nabla^2 V(x)$ .

One of the authors<sup>5</sup> proves that the above GAD (the general form (3) and the gradient form (4)) has the property that its stable critical point corresponds to an index-1 saddle point of the original dynamics,  $\dot{x} = b(x)$  or  $\dot{x} = -\nabla V(x)$ . Our simplified GAD has the exactly same property, which will be given below in details.

In the GAD (3) for non-gradient systems, both  $J(x)v$  and  $J(x)^T w$  in (3b) and (3c) must be calculated. One can apply the finite difference scheme to compute the matrix-vector multiplication  $J(x)v$ . But this trick could not be applied to the term  $J(x)^T w$ . It can only be obtained by a numerical transpose operation. The matrix-vector multiplication  $J(x)^T w$  may impose a severe computational challenge for large scale problems.

### B. Simplified GAD

Our new GAD takes *one* of the following two forms (not simultaneously):

$$\begin{cases} \dot{x} = b(x) - 2 \langle b(x), v(t) \rangle v(t) / \|v(t)\|^2, \end{cases} \quad (5a)$$

$$\dot{v} = J(x)v - \langle v, Jv \rangle v, \quad (5b)$$

or

$$\begin{cases} \dot{x} = b(x) - 2 \langle b(x), w(t) \rangle w(t) / \|w(t)\|^2, \end{cases} \quad (6a)$$

$$\dot{w} = J^T(x)w - \langle w, J^T w \rangle w. \quad (6b)$$

So, the simplified GAD is always a flow in  $\mathbb{R}^{2d}$ . Initially,  $\|v_0\| = 1$  or  $\|w_0\| = 1$  so that  $v$  and  $w$  are always unit vectors. The difference between (5) and (6) is the matrix-vector multiplication  $J(x)v$  or  $J(x)^T w$ . As discussed above, to avoid computing  $J(x)^T w$ , one prefers the equation (5) for the simplified GAD in practice. It will be seen later that in theory, equation (6) may be of more interest. For the gradient system  $\dot{x}(t) = -\nabla V(x)$ ,  $J = -H$ , where  $H = \nabla^2 V = H^T$  is the Hessian matrix, the above two forms are identical and become the GAD (4) for the gradient system.

**Remark 1.** A positive constant  $\tau$  can be used in the simplified GAD:  $\dot{v} \rightarrow \tau \dot{v}$  (or  $\dot{w} \rightarrow \tau \dot{w}$  as in equation (3)), to represent the time scale ratio between  $x$  and  $v$  (or  $w$ ). We drop this factor to ease the presentation.

The simplified GAD (5) or (6) converges to the index-1 saddle point of the original dynamics  $\dot{x} = b(x)$ ; see the following theorem. The proof is quite similar to that for the original GAD<sup>5</sup>.

**Theorem 1.** (a) If  $(x_*, v_*)$  is a fixed point of the simplified GAD (5), and  $v_*$  is the normalized vector,  $\|v_*\| = 1$ , then  $v_*$  is the eigenvector of  $J(x_*)$  corresponding to an eigenvalue  $\lambda_*$ , i.e.,

$$J(x_*)v_* = \lambda_*v_*,$$

and  $x_*$  is a fixed point of the original dynamics system, i.e.,  $b(x_*) = 0$ ;

(b) Let  $x_s$  be a fixed point of the dynamical system  $\dot{x} = b(x)$ . If the Jacobian matrix  $J(x_s)$  has  $n$  distinct real eigenvalues  $\lambda_1, \lambda_2, \dots, \lambda_n$  corresponding to the  $n$  linearly independent eigenvectors  $v_i$ , i.e.,

$$J(x_s)v_i = \lambda_i v_i, \quad i = 1, 2, \dots, n$$

and  $\|v_i\| = 1, \forall i$ . Then  $(x_s, v_i), \forall i$ , is a fixed point of the simplified GAD (5). Furthermore, there is one fixed point  $(x_s, v_{i'})$  among these  $n$  fixed points, which is linearly stable if and only if  $x_s$  is an index-1 saddle point of the original dynamical system  $\dot{x} = b(x)$  and the eigenvalue  $\lambda_{i'}$  corresponding to  $v_{i'}$  is the only positive eigenvalue of  $J(x_s)$ .

*Proof.* (a) By the condition that  $(x_*, v_*)$  is a fixed point of the simplified GAD (5), we have

$$\begin{cases} b(x_*) - 2 \langle b(x_*), v_* \rangle v_* = 0, \\ J(x_*)v_* = \langle v_*, J(x_*)v_* \rangle v_*. \end{cases} \quad (7a)$$

$$(7b)$$

Equation (7b) implies that  $v_*$  is the eigenvector of  $J(x_*)$  corresponding to the eigenvalue  $\lambda_* \doteq \langle v_*, J(x_*)v_* \rangle$ .

Making inner product with  $v_*$  on both sides of (7a), we can get

$$\langle b(x_*), v_* \rangle - 2 \langle b(x_*), v_* \rangle \langle v_*, v_* \rangle = 0.$$

Since  $\|v_*\| = 1$ , we have  $\langle b(x_*), v_* \rangle = 0$ . Thus  $b(x_*) = 0$  by (7a).

(b) Since  $x_s$  is a fixed point of the system  $\dot{x} = b(x)$ , we have  $b(x_s) = 0$ , thus

$$b(x_s) - 2 \langle b(x_s), v_i \rangle v_i / \|v_i\|^2 = 0, \quad i = 1, 2, \dots, n. \quad (8)$$

Since  $J(x_s)v_i = \lambda_i v_i$ , by taking inner product with  $v_i$  on both sides and using the condition  $\|v_i\| = 1$ , we get  $\lambda_i = \langle J(x_s)v_i, v_i \rangle$ , and

$$J(x_s)v_i - \langle J(x_s)v_i, v_i \rangle v_i = 0, \quad i = 1, 2, \dots, n. \quad (9)$$

Equation (8) and (9) imply that  $(x_s, v_i)$  is the fixed point of the simplified GAD (5) for all  $i = 1, 2, \dots, n$ .

Next, we write down the eigenvalues and corresponding eigenvectors of the Jacobian matrix of the simplified GAD at any fixed point  $(x_s, v_i)$ . First, the Jacobian matrix of the simplified GAD (5) has the following expression:

$$\tilde{\mathbb{J}}(x_s, v_i) = \begin{bmatrix} \mathbb{N}_1 := J - 2\lambda_i v_i v_i^\top, & 0 \\ *, & \mathbb{M}_1 := J - \lambda_i - v_i v_i^\top (\lambda_i + J) \end{bmatrix}. \quad (10)$$

The eigenvalues of  $\tilde{\mathbb{J}}$  can be obtained from the eigenvalues of its two diagonal blocks  $\mathbb{N}_1$  and  $\mathbb{M}_1$ . It can be verified that

$$\begin{aligned} \mathbb{N}_1 v_i &= J v_i - 2\lambda_i v_i v_i^\top v_i = -\lambda_i v_i, \\ \mathbb{N}_1 v_j &= J v_j - 2\lambda_i v_i v_i^\top v_j = \lambda_j v_j, \\ \mathbb{M}_1 v_i &= J v_i - \lambda_i v_i - v_i v_i^\top (\lambda_i + J) v_i = -2\lambda_i v_i, \end{aligned}$$

and

$$\begin{aligned} \mathbb{M}_1(v_j - (v_j^\top v_i)v_i) &= \mathbb{M}v_j - (v_j^\top v_i)\mathbb{M}v_i \\ &= (J - \lambda_i - v_i v_i^\top (\lambda_i + J))v_j + 2\lambda_i(v_j^\top v_i)v_i \\ &= (\lambda_j - \lambda_i)v_j - v_i(\lambda_i + \lambda_j)v_i^\top v_j + 2\lambda_i(v_j^\top v_i)v_i \\ &= (\lambda_j - \lambda_i)v_j - v_i(\lambda_j - \lambda_i)v_i^\top v_j \\ &= (\lambda_j - \lambda_i)(v_j - (v_i^\top v_j)v_i). \end{aligned}$$

Hence the eigenvalues of the Jacobian matrix  $\tilde{\mathbb{J}}$  at any fixed points  $(x_s, v_i), i = 1, 2, \dots, n$  are

$$-2\lambda_i, -\lambda_i, \{\lambda_j : j \neq i\}, \{\lambda_j - \lambda_i : j \neq i\}. \quad (11)$$

The linear stability condition is that all the above eigenvalues of  $\tilde{\mathbb{J}}$  are negative. Thus one fixed point  $(x_s, v_{i'})$  is linearly stable if and only if  $\lambda_{i'} > 0$  and all other eigenvalues  $\lambda_j < 0$  for  $j \neq i'$ . In this case, the fixed point  $x_s$  is an index-1 saddle point of the system  $\dot{x} = b(x)$ .  $\square$

**Remark 2.** Theorem 1 also holds for the simplified GAD (6). In this case, the Jacobian matrix of the simplified GAD (6) becomes

$$\tilde{\mathbb{J}}(x_s, w_i) = \begin{bmatrix} \mathbb{N}_2 := J - 2\lambda_i w_i w_i^\top, & 0 \\ *, & \mathbb{M}_2 := J^\top - \lambda_i - w_i w_i^\top (\lambda_i + J^\top) \end{bmatrix} \quad (12)$$

with the same eigenvalues (11) as the Jacobian matrix of the simplified GAD (5).

### C. Relation with Hamilton's equation

In this part, we discuss the Hamilton's equation associated with the rare event study of the equation (2). According to the Freidlin-Wentzell large deviation principle (LDP)<sup>6</sup>, as the noise amplitude  $\varepsilon$  in equation (2) tends to zero, the most probable transition path over the time interval  $[0, T]$  of the system (2) is the minimizer of the following Freidlin-Wentzell action functional

$$S[\phi] = \int_0^T L(\phi, \dot{\phi}) dt, \quad (13)$$

where the Lagrangian  $L(x, y)$  is defined as

$$L(x, y) := \frac{1}{2} \langle y - b(x), y - b(x) \rangle. \quad (14)$$

$\langle \cdot, \cdot \rangle$  is the inner product in  $\mathbb{R}^d$ . The Hamiltonian  $H(x, p)$ , as the conjugate of the Lagrangian  $L(x, y)$ , is

$$H(x, p) = \langle b(x), p \rangle + \langle p, p \rangle / 2. \quad (15)$$

It is well-known that the minimizer of  $S[\phi]$ , denoted as  $x(t)$ , satisfies the Hamilton's equations

$$\begin{cases} \dot{x} = H_p = b(x) + p(t), \\ \dot{p} = -H_x = -J(x)^T p(t), \end{cases} \quad (16a)$$

$$(16b)$$

where  $p(t)$  is the (generalized) momentum.  $J(x) = Db(x)$  is the Jacobian matrix we have used before in the GAD. The eigenvalues of  $J(x)$  are denoted as  $\{\lambda_i\}$ . Equation (16) looks superficially similar to equation (6) with two differences: (i) the signs before  $J(x)^T$  are the opposite and (ii) the momentum  $p$  is not a unit vector as the direction variable  $w$ . In fact, the critical point of (16) is  $(x_*, p_*)$  where  $b(x_*) = 0$  and  $p_* = 0$  by assuming that  $J(x_*)$  is non-degenerate. Assume  $J(x)$  has the right-eigenvectors  $v_i$  and the left-eigenvectors  $w_i$ :

$$Jv_i = \lambda_i v_i, \text{ and } J^T w_i = \lambda_i w_i, \quad 1 \leq i \leq d,$$

where all eigenvalues are assumed distinctive and the left or right eigenvectors both form a basis of  $\mathbb{R}^d$ . We introduce the normalized unit vector  $u$  to represent the direction of  $p$ . Define the scalar  $l \doteq \|p\|^2$ , then  $u = p/\sqrt{l}$  and  $\dot{l} = 2\langle p, \dot{p} \rangle = -2\langle p, J^T p \rangle = -2l\langle u, J^T u \rangle$ . So,

$$\dot{u} = \frac{d}{dt} \left( \frac{p}{\sqrt{l}} \right) = -J^T(x)u + \langle u, J^T u \rangle u. \quad (17)$$

By the important zero-Hamiltonian condition  $H \equiv 0$ <sup>(6)</sup>, we have

$$l = \|p\|^2 = -2\langle b, p \rangle = -2\sqrt{l}\langle b, u \rangle;$$

that is,

$$l = 0, \quad \text{or} \quad \sqrt{l} = -2\langle b(x), u \rangle.$$

$l = 0$  means  $p = 0$ , which corresponds to the original dynamics  $\dot{x} = b(x)$ .  $l$  is not always zero for the exit dynamics, then  $\sqrt{l} = -2\langle b(x), u \rangle$  and the equation (16a) becomes

$$\dot{x} = b(x) + \sqrt{l}u = b(x) - 2\langle b(x), u \rangle u. \quad (18)$$

So far, by (17) and (18), we get the momentum-normalized version for the Hamilton's equation (16) restricted on the zero- $H$  hypersurface:

$$\begin{cases} \dot{x} = b(x) - 2\langle b(x), u(t) \rangle u(t) / \|u(t)\|^2, \\ \dot{u} = -J^T(x)u + \langle u, J^T u \rangle u. \end{cases} \quad (19a)$$

$$(19b)$$

$\|u_0\| = 1$  is assumed. Note that this dynamics (19) is not exactly identical to the original Hamilton's equation (16) since the branch of  $p \equiv 0$  has been discarded.

Now, the only difference between the Hamilton's equation (19) and the simplified GAD (6) is the opposite sign on the right hand sides of (19b) and (6b). By Remark 2, the Jacobian matrix of (19) is  $\begin{bmatrix} \mathbb{N}_2 & 0 \\ *, & -\mathbb{M}_2 \end{bmatrix}$ , whose eigenvalues are  $-\lambda_i, 2\lambda_i, \{\lambda_j, j \neq i\}, \{\lambda_i - \lambda_j, j \neq i\}$ . The position dynamics in (6) and (19) have the same form of applying the projection matrix  $I - 2ww^T$  or  $I - 2uu^T$  in front of the original force  $b(x)$ . The difference is which direction they select. If  $x$  were frozen, the  $w$  dynamics in equation (6b) picks up the least stable direction while the Hamilton equation's momentum direction uses the most stable direction. Thus the GAD (6) can converge to the saddle point of the vector field  $b(x)$  while the Hamiltonian dynamics (19) has no stable steady state. So one may view the simplified GAD as a modification of the Hamilton's equation by flipping the sign of the (normalized) momentum to stabilized the saddle point. Note that although we can introduce a factor  $\gamma$  for (6b) as shown in Remark 1 to speed up the clock for the direction dynamics, there is no such a freedom for the Hamilton's equation (19b).

#### D. Application to multiscale model

The GAD was extended to the slow-fast stochastic system in<sup>9</sup> and the resulted method is called MsGAD. As a corollary of our result, the simplified GAD here can be applied to this multi-scale model straightforwardly. For the backgrounds and more details, the reader can refer to<sup>9</sup>. We here directly present the scheme based on the above simplified GAD. The slow-fast system in consideration is

$$\begin{cases} \dot{X}^\varepsilon(t) = f(X^\varepsilon, Y^\varepsilon), \\ \dot{Y}^\varepsilon(t) = \frac{1}{\varepsilon}b(X^\varepsilon, Y^\varepsilon) + \frac{1}{\sqrt{\varepsilon}}\sigma(X^\varepsilon, Y^\varepsilon)\eta(t), \end{cases} \quad (20a)$$

$$(20b)$$

where  $\varepsilon$  is a small parameter and  $\eta$  is the noisy perturbation.  $X^\varepsilon$  is the slow variable and  $Y^\varepsilon$  is the fast variable. When  $\varepsilon$  goes to zero, the effective dynamics of the slow variable is

$$\dot{\bar{X}} = F(\bar{X}), \quad \text{where } F(x) \doteq \int f(x, y)\mu_x(dy), \quad (21)$$

where  $\mu_x(dy)$  is the invariant measure of the fast process with the density function denoted by  $\rho(x, y)$ .  $F$  usually does not have analytical form. The simplified multiscale GAD for the saddle point of equation (21) is

$$\begin{cases} \dot{x}^\varepsilon(t) = f(x^\varepsilon, y^\varepsilon) - 2\frac{\langle f(x^\varepsilon, y^\varepsilon), v^\varepsilon \rangle}{\langle v^\varepsilon, v^\varepsilon \rangle}v^\varepsilon, \\ \dot{y}^\varepsilon(t) = \frac{1}{\varepsilon}b(x^\varepsilon, y^\varepsilon) + \frac{\sigma(x^\varepsilon, y^\varepsilon)}{\sqrt{\varepsilon}}\eta(t), \end{cases} \quad (22a)$$

$$(22b)$$

$$\dot{v}^\varepsilon(t) = (D_x f(x^\varepsilon, y^\varepsilon) + C(x^\varepsilon, y^\varepsilon))v^\varepsilon - \alpha^\varepsilon v^\varepsilon, \quad (22c)$$

or

$$\begin{cases} \dot{x}^\varepsilon(t) = f(x^\varepsilon, y^\varepsilon) - 2 \frac{\langle f(x^\varepsilon, y^\varepsilon), w^\varepsilon \rangle}{\langle w^\varepsilon, w^\varepsilon \rangle} w^\varepsilon, \\ \dot{y}^\varepsilon(t) = \frac{1}{\varepsilon} b(x^\varepsilon, y^\varepsilon) + \frac{\sigma(x^\varepsilon, y^\varepsilon)}{\sqrt{\varepsilon}} \eta(t), \end{cases} \quad (23a)$$

$$\dot{w}^\varepsilon(t) = (D_x f(x^\varepsilon, y^\varepsilon) + C(x^\varepsilon, y^\varepsilon))^T w^\varepsilon - \beta^\varepsilon w^\varepsilon, \quad (23b)$$

$$(23c)$$

where  $D_x f(x, y)$  is the Jacobian matrix of  $f(x, y)$  with respect to  $x$ .  $\alpha = \langle v, (D_x f + C)v \rangle$ ,  $\beta = \langle w, (D_x f + C)^T w \rangle$ ,  $C(x, y) = (f(x, y) - F(x)) \otimes (g(x, y) - G(x))$ ,  $g(x, y) = -\nabla_x U(x, y)$ ,  $U(x, y) = -\log \rho(x, y)$  and  $G(x) = \int g(x, y) \mu_x(dy)$ .

### III. NUMERICAL EXAMPLES

#### A. A two-dimensional deterministic system

The first test is to find the saddle point of the following two dimensional non-gradient system

$$\dot{x}_i = - \sum_{j=1}^2 D_{ij} x_j + \frac{\sigma^2}{2} \Gamma_i(x), \quad i = 1, 2, \quad (24)$$

where  $\sigma^2 = 10$ ,  $D = \begin{bmatrix} 0.8 & -0.3 \\ -0.2 & 0.5 \end{bmatrix}$  and  $\Gamma_i(x) = (1 + (x_i - 5)^2)^{-1}$ ,  $i = 1, 2$ . This dynamics has two stable fixed points  $m_1 = (0.5931, 0.7655)$ ,  $m_2 = (5.8770, 6.2507)$  and a unique saddle point  $s = (1.7954, 3.3088)$ . Figure 1 shows the simplified GAD trajectories of the  $x$  component (solid lines) starting from  $m_1$  and  $m_2$  respectively.

#### B. A two-dimensional slow-fast system

Consider a slow-fast system in<sup>9</sup>,

$$\begin{cases} \dot{x}_i = - \sum_j D_{ij} x_j + y_i^2, \\ \dot{y}_i = - \frac{1}{\varepsilon} \frac{y_i}{\Gamma_i(x)} + \frac{1}{\sqrt{\varepsilon}} \sigma \eta(t), \end{cases} \quad (25a)$$

$$(25b)$$

where  $D = \begin{bmatrix} 0.8 & -0.2 \\ -0.2 & 0.5 \end{bmatrix}$ , which is different from the  $D$  matrix in the first example (24).  $\sigma^2$  and  $\Gamma_i(x)$  are the same as in the first example.  $\eta$  is the standard white noise. We are interested in the saddle point of the effective dynamics which is the limit of (25) as  $\varepsilon \rightarrow 0$ . For this special case, it happens to have the following closed form for the effective dynamics

$$\dot{\bar{X}}_i = - \sum_j D_{ij} \bar{X}_j + \frac{\sigma^2}{2} \Gamma_i(\bar{X}). \quad (26)$$

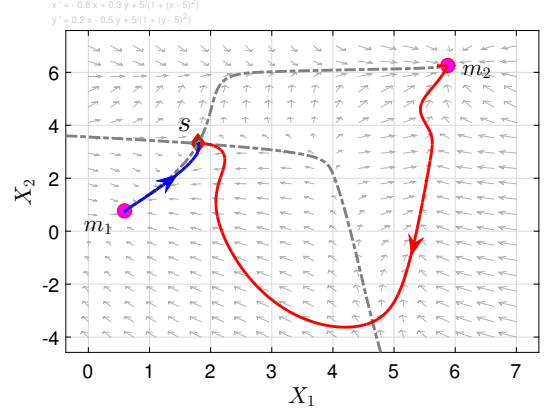


Figure 1: GAD trajectories of the  $x$  component from two locally stable fixed points ( $m_1$  and  $m_2$ ) to the saddle point  $s$ . The flow indicated by the arrows corresponds to the non-gradient system (24). The dash-dotted curves are the stable/unstable manifolds of the saddle point; they determine the basin boundaries of the two stable fixed points. The blue and red curves with arrows are the trajectories of the  $x$  component for the simplified GAD applied to the dynamics (24) with the initial vector  $v = [1, 0]$  and  $[0, 1]$ , respectively.

Equation (26) has three stable fixed points  $m_1 = (0.4643, 0.6985)$ ,  $m_2 = (2.2038, 5.9804)$  and  $m_3 = (5.7109, 6.2369)$  as well as two saddle points  $s_1 = (1.2842, 3.4484)$ ,  $s_2 = (3.5689, 6.0735)$ . Refer to Figure 2. To test our method, we use the heterogeneous multi-scale method(HMM) to solve the simplified MsGAD (22) numerically, without using any information of the analytical form in equation (26). Figure 2 shows four GAD trajectories of the  $x$  component (black solid lines) with different initial values.

#### C. Nucleation in the presence of shear flow

As the last example, we consider a more challenging problem: the nucleation in the reaction-diffusion equation in the presence of shear. Nucleation is a very important physical phenomenon<sup>11,12,14,16,22</sup> and the nucleus is usually described by the saddle point of the Ginzburg-Landau free energy. In the case of gradient systems purely driven by the free energy, the string method<sup>2,4</sup> can be applied to calculate the minimum energy path. When the shear flow field is in presence, one is faced with a non-gradient systems and in principle, one needs the minimum action method<sup>3</sup> to compute the minimum action path and the minimal action<sup>11</sup>. The saddle point can be extracted after the whole path is computed. By our new method, however, the saddle point in the shear flow case can be calculated directly. The Ginzburg-Landau

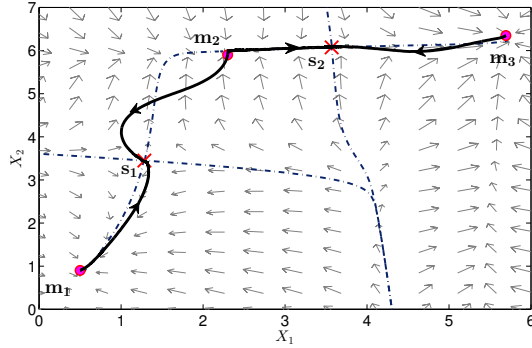


Figure 2: GAD trajectories from three stable fixed points ( $m_1, m_2$  and  $m_3$ ) to two different saddle points ( $s_1$  and  $s_2$ ). The flow indicated by the arrows corresponds to the effective dynamics (26). The dash-dotted curves are the stable/unstable manifolds of the two saddle points under the flow (26). The black solid curves with arrows marked are the trajectories of the simplified MsGAD by the HMM.

free energy of the order parameter  $\phi(x, y)$  is

$$E(\phi) = \int_{\Omega} \frac{\kappa}{2} |\nabla \phi|^2 + \frac{1}{4} (1 - \phi^2)^2 dx dy, \quad (27)$$

where  $\kappa = 0.01$ , the domain  $\Omega = [0, 1] \times [0, 1]$ . The periodic boundary condition is considered. We study two cases of the shear flow as illustrated in Figure 3, then the corresponding dynamics of the Allen-Cahn equation in the presence of the shears are

$$\partial_t \phi = -\frac{\delta E}{\delta \phi} + \gamma \sin(2\pi y) \partial_x \phi, \quad (28)$$

and

$$\partial_t \phi = -\frac{\delta E}{\delta \phi} + \gamma \sin(2\pi y) \partial_x \phi + \gamma \sin(2\pi x) \partial_y \phi, \quad (29)$$

respectively, where  $\gamma$  is the shear rate and the Fréchet derivative  $\delta_\phi E = -\kappa \Delta \phi - \phi + \phi^3$ .

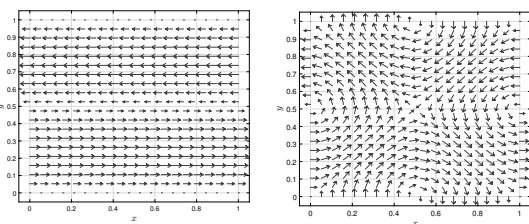


Figure 3: Vector fields of the two types of shear flows.

We want to locate the index-1 saddle point in the dynamics (28) and (29) by the simplified GAD in Section

II B. Denote the right hand side in (28) or (29) by  $b(\phi)$ , the simplified GAD (5) in this case is

$$\left\{ \begin{array}{l} \partial_t \phi = b(\phi) - 2 \langle b(\phi), v \rangle v / \|v\|^2, \\ \partial_t v = Db(\phi)v - \langle v, (Db)v \rangle v / \|v\|^2, \end{array} \right. \quad (30a)$$

$$\left\{ \begin{array}{l} \partial_t \phi = b(\phi) - 2 \langle b(\phi), v \rangle v / \|v\|^2, \\ \partial_t v = Db(\phi)v - \langle v, (Db)v \rangle v / \|v\|^2, \end{array} \right. \quad (30b)$$

where  $v = v(x, t)$  and  $\langle \cdot, \cdot \rangle$ ,  $\|\cdot\|$  is the  $L^2$  inner product and norm in space.

**Remark 3.** Here the dynamics is a PDE model and we can have the analytical expression for the Jacobian and its transpose. We take the case in equation (28) as an example to show  $Db$  and its adjoint  $(Db)^T$ .  $b(\phi) = \kappa \Delta \phi + \phi - \phi^3 + \gamma \sin(2\pi y) \partial_x \phi$ .  $Db(\phi)v = \kappa \Delta v + v - 3\phi^2 v + \gamma \sin(2\pi y) \partial_x v$ . Then  $(Db(\phi))^T w = \kappa \Delta w + w - 3\phi^2 w - \gamma \sin(2\pi y) \partial_x w$  since the adjoint of  $\partial_x$  is  $-\partial_x$ . This example shows that when  $b$  is a differential operator, one may obtain the “transpose” (adjoint) of the Jacobian analytically. Then the two forms of the simplified GAD (5) and (6) are both applicable in such cases.

In the numerical test, we use the mesh point  $N_x = N_y = 128$  in the finite difference method for spatial discretization. The two metastable states are always  $\phi \equiv 1$  and  $\phi \equiv -1$  regardless of the shear flow. By solving the simplified GAD (30), we get different index-1 saddle points for various  $\gamma$ . We are interested in the impact of shear flow on the profiles of the saddle point. It is noted that the steady states for any shear preserve the symmetry  $\phi \rightarrow -\phi$  and equation (29) additionally preserves the second symmetry  $\phi(x, y) \rightarrow \phi(y, x)$ . So there are multiple symmetric images for the same steady states. All of our plots below show only one of the symmetric images.

For the first case in equation (28), the shear force exists only in the  $x$  direction. As  $\gamma$  increases, the sequence of the profiles of the saddle point is shown in Figure 4. We have the following interesting observations from this figure: the profiles of the saddle points get more and more stretched along the shear direction until a lamellar phase is attained for  $\gamma$  large enough. In fact, the lamellar phase shown in the last two subfigures (Figure 4e and 4f) is always a saddle point for any value of  $\gamma$ . It seems to have a critical  $\gamma_*$  between 0.05 and 0.065 such that for  $\gamma < \gamma_*$ , there are two saddles: one is twisted and the other is lamellar, and for  $\gamma > \gamma_*$ , it seems only one index-1 saddle point, the lamellar phase. To determine which saddle point has the minimal action of escape a metastable state for a specific  $\gamma < \gamma_*$ , one needs to further run the minimum action method as in<sup>11</sup>.

For the second shear case in equation (29), the shear flow is no longer restricted in certain direction and is more general. In this case, the transition states with various shear rates are shown in Figure 5. The shear “twists” the profiles again but in different patterns. Similarly to the first case, the saddle point is finally unchanged when  $\gamma$  is sufficiently large. And eventually, the saddle point forms an “X” shape. But for small shear rate, the “X” shaped saddle point in Figure 5f does not exist, unlike the lamellar phase in the previous shear case. Thus, it seems

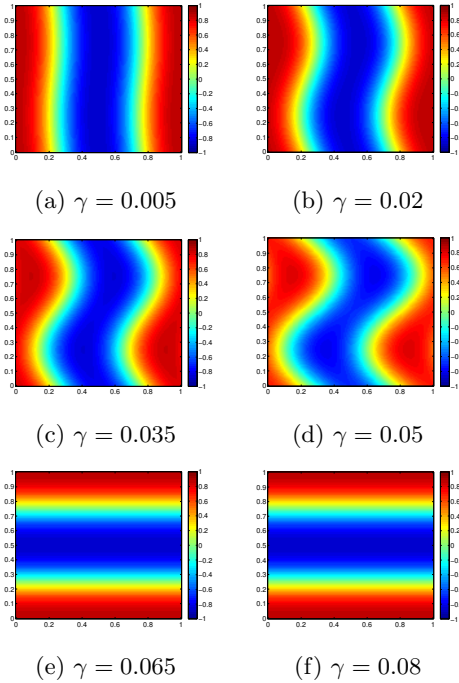


Figure 4: Saddle points for the model (28).

to have only one index-1 saddle point at any  $\gamma$ , except for the symmetric images. In summary, the shear acting on the Ginzburg-Landau energy landscape induces a variety of different patterns of the saddle points and transition mechanisms. Our simplified GAD offers a useful tool for locating these saddle points with economic computational costs.

#### IV. CONCLUDING REMARKS

We present a simplified GAD for the non-gradient system in  $\mathbb{R}^d$  to search saddle points. It is a flow in  $\mathbb{R}^{2d}$  rather than in  $\mathbb{R}^{3d}$ . Only one direction variable and one position variable are required in this new GAD. So, it has the same computational cost as the GAD for the gradient system. Although we only show the result for index-1 saddle points in this paper, it is not difficult to extend to index- $k$  saddle points by following the approach in the original GAD paper<sup>5</sup>.

Our numerical tests include the Allen-Cahn equation in a periodic box with the presence of shear flow and we find the changes of saddle points when the system is subject to the various shear flows. In the end, we need to point out that although index-1 saddle points seem important for the rare-event transitions in the non-gradient systems, the saddle point found by the GAD may not directly be the true transition state. To quantify the minimal action, the minimum action method may still be necessary to evaluate the action to the saddle points. One may combine the MAM for the path and the

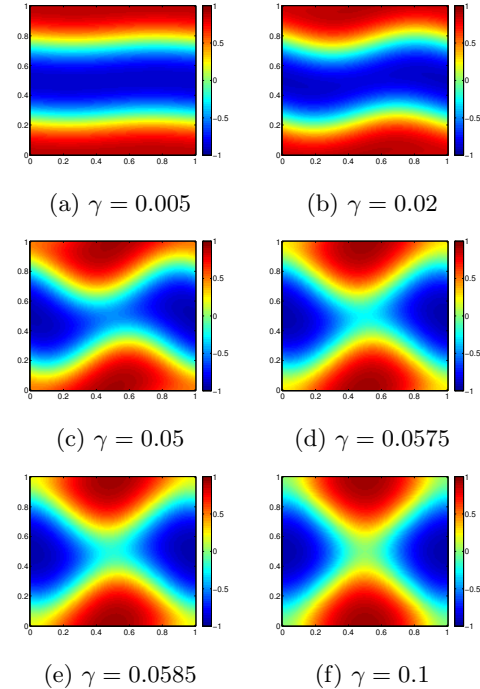


Figure 5: Saddle points for the model (29).

GAD for the final ending point on the path to construct a hybrid method, in a similar style to the climbing string method<sup>15</sup> for the gradient system.

#### REFERENCES

- <sup>1</sup>G. M. CRIPPEN AND H. A. SCHERAGA, *Minimization of polypeptide energy : XI. the method of gentlest ascent*, Arch. Biochem. Biophys., 144 (1971), pp. 462–466.
- <sup>2</sup>W. E, W. REN, AND E. VANDEN-EIJNDEN, *String method for the study of rare events*, Phys. Rev. B, 66 (2002), p. 052301.
- <sup>3</sup>W. E, W. REN, AND E. VANDEN-EIJNDEN, *Minimal action method for rare events*, Commun. Pure Appl. Math., 57 (2004), pp. 637–656.
- <sup>4</sup>W. E, W. REN, AND E. VANDEN-EIJNDEN, *Simplified and improved string method for computing the minimum energy paths in barrier-crossing events*, J. Chem. Phys., 126 (2007), p. 164103.
- <sup>5</sup>W. E AND X. ZHOU, *The gentlest ascent dynamics*, Nonlinearity, 24 (2011), p. 1831.
- <sup>6</sup>M. I. FREIDLIN AND A. D. WENTZELL, *Random Perturbations of Dynamical Systems*, Grundlehren der mathematischen Wissenschaften, Springer-Verlag, New York, 3 ed., 2012.
- <sup>7</sup>W. GAO, J. LENG, AND X. ZHOU, *An iterative minimization formulation for saddle point search*, SIAM J. Numer. Anal., 53 (2015), pp. 1786–1805.
- <sup>8</sup>\_\_\_\_\_, *Iterative minimization algorithm for efficient calculations of transition states*, J. Comput. Phys., 309 (2016), pp. 69–87.
- <sup>9</sup>S. GU AND X. ZHOU, *Multiscale gentlest ascent dynamics for saddle point in effective dynamics of slow-fast system*, Commun. Math. Sci., 15 (2017), pp. 2279–2302.
- <sup>10</sup>G. HENKELMAN AND H. JÓNSSON, *A dimer method for finding saddle points on high dimensional potential surfaces using only first derivatives*, J. Chem. Phys., 111 (1999), pp. 7010–7022.
- <sup>11</sup>M. HEYMANN AND E. VANDEN-EIJNDEN, *Pathways of maximum*

- likelihood for rare events in nonequilibrium systems: Application to nucleation in the presence of shear*, Phys. Rev. Lett., 100 (2008), p. 140601.
- <sup>12</sup>L. LIN, X. CHENG, W. E, A. SHI, AND P. ZHANG, *A numerical method for the study of nucleation of ordered phases*, J. Comput. Phys., 229 (2010), pp. 1797–1809.
- <sup>13</sup>N. MOUSSEAU AND G. BARKEMA, *Traveling through potential energy surfaces of disordered materials: the activation-relaxation technique*, Phys. Rev. E, 57 (1998), p. 2419.
- <sup>14</sup>A. ONUKI, *Phase transitions of fluids in shear flow*, J. Phys.: Condens. Matter, 9 (1997), pp. 6119–6157.
- <sup>15</sup>W. REN AND E. VANDEN-EIJNDEN, *A climbing string method for saddle point search*, J. Chem. Phys., 138 (2013), p. 134105.
- <sup>16</sup>A. ROY, J. M. RICKMAN, J. D. GUNTON, AND K. R. ELDER, *Simulation study of nucleation in a phase-field model with nonlocal interactions*, Phys. Rev. E, 57 (1998), pp. 2610–2617.
- <sup>17</sup>A. SAMANTA AND W. E, *Atomistic simulations of rare events using gentlest ascent dynamics*, J. Chem. Phys., 136 (2012), p. 124104.
- <sup>18</sup>D. J. WALES, *Energy Landscapes with Application to Clusters, Biomolecules and Glasses*, Cambridge University Press, 2003.
- <sup>19</sup>X. WAN, H. YU, AND W. E, *Model the nonlinear instability of wall-bounded shear flows as a rare event: a study on two-dimensional Poiseuille flow*, Nonlinearity, 28 (2015), p. 1409.
- <sup>20</sup>X. WAN, X. ZHOU, AND W. E, *Study of noise-induced transition and the exploration of the configuration space for the Kuramoto-Sivashinsky equation using the minimum action method*, nonlinearity, 23 (2010), pp. 475–493.
- <sup>21</sup>J. ZHANG AND Q. DU, *Shrinking dimer dynamics and its applications to saddle point search*, SIAM J. Numer. Anal., 50 (2012), pp. 1899–1921.
- <sup>22</sup>L. ZHANG, L. Q. CHEN, AND Q. DU, *Morphology of critical nuclei in solid state phase transformations*, Phys. Rev. Lett., 98 (2007), p. 265703.